Defence Research and Development Canada
Recherche et développement pour la défense Canada

DEFENCE R&D DÉFENSE

Distortion in ISAR Imaging and Restoration of Distorted ISAR Images

S. Wong, G. Duff and E. Riseborough

Defence R&D Canada – Ottawa
TECHNICAL MEMORANDUM
DRDC Ottawa TM 2003-143
September 2003

Canada

Distortion in ISAR Imaging and Restoration of Distorted ISAR Images

S. Wong
DRDC Ottawa

G. Duff
DRDC Ottawa

E. Riseborough
DRDC Ottawa

Defence R&D Canada – Ottawa

Technical Memorandum

DRDC Ottawa TM 2003-143

September 2003

Abstract

A physics based numerical model has been developed to describe the gross distortion on ISAR images due to small perturbed target motion. Quantitative results obtained under controlled experimental conditions on the target's motion have confirmed that large distortion in the ISAR image of the target can occur. The experimental data give excellent agreement with the model results. The distortion is a consequence of the phase modulation effect in the radar return signal, as a result of small fluctuating perturbed motion of the target. This gives rise to distortion of the image in the cross-range direction. The distortion can be corrected by applying time-frequency analysis. The Short-Time Fourier transform is used in this paper to examine some of the issues in refocusing distorted ISAR images.

Résumé

Le présent rapport traite des expériences menées sur la distorsion brute des images ISAR, qui est causée par un faible mouvement perturbateur des cibles. Les résultats quantitatifs obtenus dans des expériences sur le mouvement des cibles, menées dans des conditions contrôlées, démontrent que l'image ISAR d'une cible peut subir une grande distorsion. Cette distorsion est causée par l'effet de modulation de phase de l'écho radar suite à un faible mouvement perturbateur fluctuant des cibles. Cela entraîne une distorsion de l'image sur le plan transversal. Une analyse temps-fréquence permet de corriger cette distorsion. Dans la présente étude, on a utilisé la transformée de Fourier fenêtrée pour résoudre certaines questions relatives à la mise au point des images ISAR déformées.

This page intentionally left blank.

Executive summary

Target identification is a critical function for command and control systems. Reliable identification of hostile targets is a crucial issue in surveillance missions and in combat situations. Although cooperative techniques such as Identification Friend or Foe are already operational for identifying friendly targets, such systems do not provide positive identification of hostile and neutral targets. Non-Cooperative Target Recognition (NCTR) techniques are recognized as potential solutions for obtaining reliable hostile target identification. Furthermore, target identification will be an integral part of a new approach to battlespace information management. The ability to identify targets will allow the Canadian Forces to obtain a better situational awareness of the environment surrounding the battlespace, to engage potentially threatening target quickly and to reduce fratricide in combat.

Inverse Synthetic Aperture Radar (ISAR) is a NCTR technique that is currently being investigated for target identification by the Combat ID community. ISAR provides a 2-dimensional radar image of a moving target. It has long-range capability, day and night under all weather conditions. The ability to identify moving targets makes ISAR an attractive operational radar mode for surveillance radar systems such as those installed on board the CP-140 long-range patrol aircraft, and for air defence radar systems such as the Active Phased Array Radar (APAR) designed for the Canadian Patrol Frigates.

To better understand the imaging physics and processing of ISAR images, the US Office of Naval Research has sponsored a research project to study the distortion of ISAR images under the Navy's International Collaborative Opportunity Program (NICOP). Canada is a participant in this project on "Time-frequency processing for ISAR imaging and Non-Cooperative Target Identification". This report describes the results of a modelling/experimental investigation performed by DRDC-Ottawa under the NICOP project.

Often, the maneuvering nature of moving targets, especially in-flight aircraft, can cause the ISAR images of the targets to distort, thus hindering the target identification process. Small random perturbing motion from moving targets can introduce severe distortion (i.e., blurring). It is very difficult to conduct a definitive study on the blurring phenomenon using real targets of opportunities. We have designed and built a target motion simulator and conducted a set of controlled experiments. A numerical model has also been developed to simulate the distortion in ISAR images due to time-dependent perturbing motion that occur in real targets. The experimental data are then used to validate the numerical model. We have successfully collected a large amount of good quality experimental ISAR images and have shown that the numerical model provides an accurate description of the ISAR distortion process. For target identification applications, the blurred images must be re-focused to obtain a clear image. Issues and procedures on how best to refocus a blurred image are discussed based on the new insights gained from the experimental and modelling work. A time-frequency analysis using the Short Time Fourier transform is performed to illustrate the re-focusing process.

Wong, S., Duff, D., Riseborough, E. 2003. Distortion in ISAR Imaging and restoration of Distorted ISAR Images. DRDC Ottawa TM 2003-143 Defence R&D Canada - Ottawa.

Sommaire

L'identification des cibles est une fonction critique des systèmes de commandement et de contrôle. La fiabilité de l'identification des cibles hostiles est une question cruciale lors des missions de surveillance et des situations de combat. Bien qu'une technique coopérative d'identification ami-ennemi soit déjà utilisée pour l'identification des cibles amies, elle ne permet pas d'identifier positivement les cibles neutres ou hostiles. Les techniques de reconnaissance de cible non coopérative (NCTR) ont été reconnues comme des solutions potentielles pour l'identification fiable des cibles hostiles. De plus, l'identification des cibles fera partie intégrante d'une nouvelle méthode de gestion de l'information sur l'espace de combat. La capacité d'identifier les cibles fournira aux Forces canadiennes une meilleure vue d'ensemble de l'environnement entourant l'espace de combat et leur permettra d'attaquer rapidement les cibles présentant une menace potentielle et de réduire les tirs fratricides durant les combats.

Le radar à synthèse d'ouverture inverse (ISAR) est employé dans une technique NCTR d'identification des cibles qui est actuellement à l'étude par les spécialistes en identification de combat. L'ISAR fournit une image radar bidimensionnelle d'une cible en mouvement. Ce radar est doté d'une fonction d'imagerie longue portée et peut fonctionner le jour comme la nuit dans toutes les conditions météorologiques. Sa capacité d'identifier les cibles en mouvement fait de l'ISAR un radar opérationnel intéressant pour l'utilisation dans les systèmes radar de surveillance, comme ceux qui sont installés à bord des aéronefs de patrouille à long rayon d'action CP-140, et dans les systèmes radar surface-air, comme les systèmes radar à balayage électronique actif (APAR) des frégates canadiennes de patrouille, conçus pour la défense contre les menaces aériennes.

Afin de mieux comprendre les propriétés physiques d'imagerie et le traitement des images de l'ISAR, l'organisme Office of Naval Research des États-Unis parraine un projet de recherche sur l'étude de la distorsion des images ISAR, qui fait partie du programme NICOP (Navy's International Collaborative Opportunity Program). Le Canada a été sélectionné pour participer au projet sur le traitement temps-fréquence de l'imagerie ISAR et l'identification des cibles non coopératives. Le présent rapport décrit les résultats de la modélisation/étude expérimentale réalisée par RDDC Ottawa dans le cadre du projet NICOP

Souvent, le type de manœuvres des cibles en mouvement, particulièrement ceux effectués par les aéronefs en vol, peut entraîner une distorsion des images ISAR des cibles et, par conséquent, nuire au processus d'identification des cibles. De faibles mouvements perturbateurs aléatoires des cibles en mouvement peuvent causer une grande distorsion (c.-à-dire une image floue). La réalisation d'une étude définitive sur le phénomène de flou au moyen de cibles inopinées réelles est très difficile. Nous avons conçu et construit un simulateur de mouvements des cibles et réalisé une série d'expériences contrôlées. Un modèle numérique a également été élaboré pour simuler la distorsion des images ISAR causée par les mouvements perturbateurs de vraies cibles, qui sont dépendants du temps. Les données de l'expérience ont ensuite été utilisées pour valider le modèle numérique. Nous avons réussi à recueillir un grand nombre d'images ISAR expérimentales de bonne qualité et à démontrer que le modèle numérique décrit avec exactitude le processus de distorsion des images ISAR.

Afin de pouvoir être utilisées dans des applications d'identification des cibles, les images floues doivent être mises au point jusqu'à obtention d'images claires. Le rapport aborde également les questions relatives aux images floues et la meilleure méthode à utiliser pour leur mise au point; cette méthode repose sur les derniers résultats des expériences et des travaux de modélisation. Une analyse temps-fréquence a également été réalisée au moyen de la transformée de Fourier fenêtrée afin d'illustrer le processus de mise au point.

Wong, S., Duff, D., Riseborough, E. 2003 Distortion in ISAR Imaging and restoration of Distorted ISAR Images. DRDC Ottawa TM 2003-143 R & D pour la défense Canada - Ottawa.

Table of contents

List of figures

Acknowledgements

The authors would like to thank Mr. Denis Lamothe for his technical support in the measurement trial in France

This page intentionally left blank.

1. Introduction

Inverse Synthetic Aperture Radar (ISAR) imaging provides a 2-dimensional radar image of a target. A 2-dimensional picture can potentially offer crucial distinctive information about the features of the target and hence it provides improved discrimination that can lead to a more accurate target identification. However, ISAR imaging relies on the target's own motion, which can be quite complex, such as the motion of a fast, maneuvering jet aircraft. As a result, severe distortion can occur in the ISAR image of the target [1]. It has been recognized that a time-varying Doppler shift due to perturbed motion in the rotation of the target is responsible for the image blurring [2]. The distortion is attributed to a phase modulation effect resulting from coherent processing of the radar signal returned from the target[3]. Significant distortion in the ISAR image is demonstrated in controlled experiments in which a small fluctuating motion is imposed on a target. A numerical model is developed to simulate the observed distortion. The model provides new insights into the mechanism of the distorting process.

For target recognition applications, the blurred ISAR image must be refocused to provide a clear image of the target for identification. We will discuss how an optimum refocused image can be obtained quickly and efficiently from the distorted image by applying the insights obtained from the experimental and numerical studies described in this paper. In essence, a time-frequency analysis is applied to a blurred ISAR image to reconstruct a focused image. We will use the Short-Time Fourier transform to illustrate the reconstruction process.

2. A Physical Description of the ISAR Distortion Process

The phase of the radar return signal from a scatterer on a moving target is given by ,

$$\phi = \frac{4\pi f}{c}\left(R - vt - X(t)\right) \tag{1}$$

where f is the transmitting radar frequency, R is the initial distance of the scatterer on the target from the radar at the on-set of the radar imaging scan, v is the radial velocity of the target and X(t) is the displacement due to the rotation of the target along the radar's line of sight. For simplicity, we consider either a stationary target or perfect translational motion compensation such that v can be set to zero. In other words, we focus only on the rotational aspect of the target in forming the ISAR image.

Consider a scatterer on a 2-dimensional target with a pair of coordinates (x_0 , y_0) with respect to the center's rotation initially at time t_0 . A change in the scatterer's coordinates due to rotation at a later time t is given by

$$\begin{pmatrix} x(t) \\ y(t) \end{pmatrix} = \begin{pmatrix} \cos(\omega(t)t) & -\sin(\omega(t)t) \\ \sin(\omega(t)t) & \cos(\omega(t)t) \end{pmatrix} \begin{pmatrix} x_0 \\ y_0 \end{pmatrix} \tag{2}$$

Hence, the displacement along the radar's line of sight X(t) = x(t) x_0 due to a rotation of the target is given by

$$X(t) = \left(x_0 \cos(\omega(t)t) - y_0 \sin(\omega(t)t)\right) - x_0 \tag{3}$$

Note that in order to describe a small fluctuation in the rotational motion, the rotational rate is written as a function of time, i.e., ω(t). That is to say, the temporal variation in the angular rotational rate is important for describing the ISAR distortion properly. A fluctuating motion can be superimposed on a constant rotation to generate distortion in the ISAR image; i.e.,

$$\omega(t) = \omega_c + \omega_r \sin(2\pi\ \Omega t) \tag{4}$$

where ω_r is the rotational amplitude, which is a function of Ω; i.e., $\omega_r(\Omega)$ and its value increases with an increasing Ω. A simple sinusoidal motion is chosen here for simplicity. However, a realistic random fluctuating motion can be accurately described using a Fourier series, containing many sinusoidal terms [3].
To generate an ISAR image, a sequence of M consecutive HRR profiles is used. Each HRR profile has N range bins. Assuming the HRR profiles are range aligned and phase aligned among one another, a Fourier transform is performed at each down-range bin of

the M HRR profiles to generate the cross-range bins. A matrix of M by N elements of cross-range and down-range bins are then used to construct the ISAR image.

For the purpose of describing the ISAR distortion process, it is more convenient to use the step-frequency version of the HRR profile representation; i.e.,

$$H_l = \frac{1}{N} \sum_{i=0}^{N-1} A_i \exp\left[j \left(\frac{4\pi f_i}{c} (R - X(t)) \right) \right] \exp\left[j \frac{2\pi}{N} l i \right] \qquad (5)$$

where the subscript l is the range-bin index, $0<l<$ N-1. N is the number of range bins. A_i is the amplitude of the frequency-domain signal response of a scatterer on the target; the subscript i is the frequency step index. Our experimental data were collected using a continuous FM-modulated waveform. Since the radar pulse repetition rate used is relatively high, i.e., 2 kHz, the modulated waveform can be closely approximated by the continuous discrete frequency coding[4]. Hence, the step frequency notation can be used to describe the HRR profile. The step frequency form is also preferred for the numerical model.

In order to give a better illustration of the principle mechanism in the ISAR distortion process, we first make a simplifying assumption that the frequency domain signal responses, A_i for i = 0, ..., N-1 are identical in Equation (5). Then, Equation (5) can be rewritten as,

$$H_l = \frac{A}{N} \sum_{i=0}^{N-1} \exp\left[j \left(\frac{4\pi (f_0 + i\Delta f)}{c} (R - X(t)) \right) \right] \exp\left[j \frac{2\pi}{N} l i \right] \qquad (6)$$

where f_0 is the initial transmitting radar frequency; Δf is the frequency step size. The radar's transmitting bandwidth is given by $(N-1)\Delta f$. Using the geometric series identity,

$$\sum_{i=0}^{N-1} \exp[j (\alpha i)] = \frac{\sin(\frac{N\alpha}{2})}{\sin(\frac{\alpha}{2})} \exp\left[j \frac{(N-1)}{2} \alpha \right] \qquad (7)$$

the HRR profile in Equation (6) can be expressed as

$$H_l = \frac{A}{N} \frac{\sin(\frac{N\alpha}{2})}{\sin(\frac{\alpha}{2})} \exp[j(\beta + \gamma R)] \exp[- j \gamma X(t)] \qquad (8)$$

where

$$\beta = \frac{(N-1)}{N}\,\pi\, l$$
$$\gamma = \frac{4\,\pi}{c}\left[\, f_0 + \frac{(N-1)}{2}\,\Delta f \,\right] \tag{9}$$
$$\alpha = \frac{2\,\pi}{N}\left[\, \frac{2}{c}(R - X(t))\, N\Delta f + l \right]$$

The magnitude of the HRR profile of the scatterer is given by

$$|H_l| = \frac{A}{N}\left|\frac{\sin(\frac{N\alpha}{2})}{\sin(\frac{\alpha}{2})}\right| \tag{10}$$

The first phase factor in equation (8), exp[j(β + γR)] determines the location of the scatterer's peak within the HRR's unambiguous range window. The term that is of particular interest is the second phase factor containing the temporal rotational motion; i.e.,

$$\begin{aligned}\psi(t) &= \exp[\, -j\,\gamma\, X(t)\,] \\ &= \exp[-j\,\gamma\,(\,(\,x_0\cos(\omega(t)t) - y_0\sin(\omega(t)t)\,) - x_0\,)\,]\end{aligned} \tag{11}$$

We want to show that the distorting effect in the ISAR image of the scatterer is a result of a time-dependent rotational motion. Under the small-rotation regime (i.e., $\sin(\omega(t)t \cong \omega(t)t$) and using a simplified geometry for the scatterer on a target as illustrated in Figure 1 (i.e., $x_0 = 0$), Equation (11) can be rewritten as

$$\psi(t) = \exp\left[\, j\,\gamma\, y_0 \int \omega(t)\, dt \,\right] \tag{12}$$

Substituting ω(t) from Equation (4) into Equation (12),

$$\begin{aligned}\psi(t) &= \exp\left[\, j\,\gamma\, y_0 \int(\,\omega_c + \omega_r \sin(2\pi\,\Omega t)\,)\, dt \,\right] \\ &= \exp\left[\, j\,\gamma\, y_0\, \omega_c \int dt \,\right]\exp\left[\, j\,\gamma\, y_0\, \omega_r \int \sin(2\pi\,\Omega t)\, dt \,\right]\end{aligned} \tag{13}$$

The first factor corresponds to a constant rotation of the target, providing a Doppler shift that allows the placement of the scatterer along the cross-range axis to form an undistorted ISAR image in the absence of any fluctuating motion. The second factor describes the phase modulation effect due to a small fluctuating motion of the scatterer that can introduce distortion. To see how the phase modulation effect comes about more clearly, the second phase factor in Equation (13) can be rewritten as,

$$\mu(t) = \exp\left(\, j\gamma\, y_0 \omega_r \int \sin(\,2\pi\,\Omega t)\, dt \right) \tag{14}$$

$$
\begin{aligned}
&= \exp(-j\ k\ \sin(\eta)) \\
&= \cos(k\sin(\eta)) - j\sin(k\sin(\eta)) \\
&= (J_0(k) + 2J_2(k)\cos(2\eta) + 2J_4(k)\cos(4\eta) + \ldots) \\
&\quad - j(2J_1(k)\sin(\eta) + 2J_3(k)\sin(3\eta) + 2J_5(k)\sin(5\eta) + \ldots)
\end{aligned}
$$

where

$$
\begin{aligned}
k &= \gamma\ \ y_0 \\
\eta &= \sin^{-1}\left[-\omega_r \int \sin(2\pi\,\Omega\, t)\, dt \right]
\end{aligned}
\qquad (15)
$$

and the J_s are the Bessel functions. It can be seen that the phase of a time-dependent rotational motion consists of many higher order sideband components. Note that this phase factor $\mu(t)$ is dependent on the motion parameters ω_r and Ω of the target. Substituting Equations (10), (13) and (14) into Equation (8) gives,

$$
H_l = |H_l|\ \exp(j\,\xi)\ \exp(j\,\mu) \qquad (16)
$$

where $\xi = \gamma\ y_0 \omega_c dt$. At each range-bin index l, for $l = 0, \ldots, N-1$, a Fourier transform is performed to generate an ISAR image; i.e.,

$$
I_{m,l} = \sum_{k=0}^{M-1} |H_{l,k}|\ \exp[\ j\ \xi_k\ ]\ \exp[j\ \mu_k\ ]\ \exp\left[\ j\ \frac{2\pi}{M}\ m\,k\ \right] \qquad (17)
$$

where the subscript m is the cross-range index, m=0, ... M-1. M is the number of HRR profiles used. The higher order Bessel components in $\mu(t)$ in Equation (14) have been shown to give rise to severe distortion in radar images [3]. It will be shown, both experimentally and numerically, in the following sections that this phase modulation has a profound effect in producing distortion in the ISAR image of a target. As a note, it should be pointed out that in the numerical model, the HRR profile as given by Equation (5) is used because the signal response A_i can be a different value at different frequencies for a real target. Furthermore, the time-dependent displacement X(t) due to the rotational motion as given by Equation (11) is used. This enables us to describe and simulate a target with multiple scatterers and at any orientation with respect to the radar.

3. Experimental Results

To study the distorting effect in ISAR images, a delta-wing shaped target was designed and built. Six trihedral reflectors were mounted on the apparatus as scattering sites on the target. A picture of the target is shown in Figure 2. The delta-wing target measured 5 m on each of its three sides. The trihedral reflectors have a length of 0.5 m on each of the sides. All six of the reflectors were connected by a set of pulleys such that when the target was rotating, all six reflectors turned and remained pointing towards the radar at all times. The motion of the delta-wing target was provided by a programmable motor drive. The target was placed approximately 2 km from the radar. Data were collected from a radar system that employed a continuous FM-modulated waveform at X-band with a 300 MHz bandwidth, centered at 10.1 GHz. A radar pulse repetition rate (PRF) of 2 kHz was used. Each HRR profile was generated in 0.5 ms (i.e., 1/PRF) and each profile had 1024 range bins.

To obtain an un-distorted ISAR image, a constant rotation rate ω_c of 1.4 degrees per second was applied to the target. The ISAR image of the target has a down-range resolution,

$$\Delta r_d = \frac{c}{2B} \tag{18}$$

and a cross-range resolution,

$$\Delta r_c = \frac{c}{2f}\,\frac{1}{\omega_c}\,\frac{PRF}{M} \tag{19}$$

Given a band-center radar frequency f = 10.1 GHz, a radar bandwidth B=300 MHz, PRF = 2 kHz, ω_c = 0.024 radian/s (i.e., 1.4 degrees/s) and M = 2000 HRR profiles (i.e., image integration time, T= M/PRF = 1s), the down-range resolution is Δr_d = 0.5 m and the cross-range resolution is Δr_c = 0.6 m. Figure 3 shows an undistorted ISAR image of the target from the measured data. The six trihedral reflectors can be seen clearly.
An additional fluctuating motion was then superimposed on top of the constant rotation. The target's fluctuating motion was measured using an optical sensor that monitored the shaft movement of the target's turn-table. Calibration of the optical sensor for small perturbing motion was very difficult, resulting in an error in the measurement of at least plus or minus 0.5 degree/s. Furthermore, the inertia of the target and backlash in the gearing system that provided the target's motion also prevent the optical sensor from providing an accurate recording of the target's position as a function of time. Instead, information on the actual motion of the target was extracted by computing a time-frequency spectrogram using a Short Time Fourier transform on the distorted ISAR image of a particular scatterer on the target. By assuming that the target acts essentially as a rigid body, the motion of one of the scatterers on the target serves as a good indicator of the motion of the target as a whole. The scatterer used in the time-frequency spectrogram corresponds to the scatterer labeled S_B located in the bottom of the undistorted ISAR image in Figure 3.

The observed temporal motion of the scatterer is shown in Figure 4a. It represents the position of the scatterer along the cross-range direction as a function of time. Since the scatterer's position in the cross-range direction is related to its Doppler velocity, the spectrogram provides, in essence, the instantaneous angular rotational velocity of the target. A corresponding digitized trace of the motion with the angular rotational rate estimated from the motion sensor data is shown in Figure 4b. The target was initially rotating at a constant angular velocity. At about the 0.5 second mark in Figure 4b, an oscillating motion was introduced. The oscillating frequency was about 1 Hz. About 2 oscillating cycles are recorded as shown in Figure 4. Because of the inertia of the target due to its considerable size and weight, and backlash in the gear meshing between the motor drive and the turn-table, the actual oscillating motion of the target was a somewhat deformed sinusoid. Using scatterer S_B to represent the target as a whole, Figure 5 shows the angular displacement of the target as a function of time. The straight dashed line represents the case when the target has a constant rotation of 1.4 degrees/s. This corresponds to an un-distorted ISAR image of the target as shown in Figure 3. The solid line represents the temporal angular movement of the target under an oscillating motion as given in Figure 4b. It can be seen from Figure 5 that the target's angular displacement deviates less than one degree from a straight line at any given time during the 3-second interval. For a target that is 5m in size, a one degree deviation produces a very small perturbed motion on the target. As an example, scatterer S_B jiggles back and forth about 5 cm for a 1-degree deviation. The solid line drifts gradually away from the dashed line in Figure 5 due to an effective increase in the average rotational velocity. This is caused by an uneven oscillating motion as evident in Figure 4b. Figure 6a shows a measured ISAR image by integrating over a one-second interval from point A to point B in Figure 4b. Figure 7a shows a measured ISAR image integrated from point B to point C in Figure 4b. Clearly, significant distortion occurred in the ISAR images of the target when the target was subjected to a fluctuating motion. Figure 8a shows an ISAR image integrated over the entire 3-second interval in Figure 4. Note that the cross-range resolution is noticeably finer in Figure 8a; this is because of the longer image integration time (i.e., 3 seconds).

4. Numerical Simulations

A numerical model of the distortion in ISAR images has been developed based on the description given in Section 2.0. The experimentally observed temporal motion as shown in Figure 4b is used as input into the model. The resulting ISAR images computed by the numerical model are shown in Figures 6b, 7b and 8b. Significant distortions are predicted by the model and the amount of distortion predicted compares quite well with the measured data, i.e., comparing with Figures 6a, 7a and 8a respectively. There are some differences between the measured and computed ISAR images visually. One explanation is that the model assumes all the scatterers on the target act as perfect rigid-bodies. On the real target, the trihedral reflectors were not rigidly mounted; they were loosely slotted into bearing brushings so that they could rotate freely. The oscillating motion, along with the plasticity (i.e., not perfectly rigid) of the target could likely result in some small extraneous motions acting on the scatterers, thus affecting the ISAR images. To give a more quantitative comparison, a slice of the cross-range intensity profile from the blurred scatterer S_B is taken from Figures 8a and 8b, at down-range bin 22. A comparison of the cross-range distorted width between the measured and computed profiles is shown in Figure 9. It can be seen that the widths of the blurred scatterer compares quite well between the measured and computed cross-range profiles.

The distortion in the ISAR images when the target possesses a small perturbed motion can be attributed to the phase modulation effect. This is demonstrated by the good agreement obtained between the simulated and measured data. Furthermore, the measured ISAR images in Figures 7a and 8a indicate that the size of the distortion is more directly correlated to the magnitude of the instantaneous Doppler velocity encountered during the image integration time interval. In Figure 7a, even though the image integration time is 1 second, the target encountered the largest variation in the Doppler motion during that integration period (i.e., the duration between B to C in Figure 4b). Hence, the distortion in the ISAR image is the same as in the case when the image was integrated over 3 seconds as shown in Figure 8a. The distortions in the measured ISAR images as illustrated in Figures 7a and 8a suggest that the phase modulation effect due to the instantaneous Doppler motion of the target provides a much more accurate description of the distorting phenomenon. This is clearly demonstrated in the simulated ISAR images as shown in Figures 6b, 7b and 8b.

It should be pointed out that the phase modulation effect produces a much worse distortion than the commonly known quadratic distortion effect [4]. The quadratic distortion is a consequence of a circular motion of the target, resulting in a non-constant Doppler velocity component along the radar's line of sight. The number of cross-range bin migration is given by

$$Z = \frac{\frac{L}{2}(\omega_c t)}{\Delta r_c} = \frac{L}{2}\frac{2f}{c}(\omega_c t)^2 \qquad (20)$$

where Δr_c is the cross-range resolution as given by Equation (19). Given that the target's length L = 5 m , the target's rotational rate $|\omega_c|_{max}$ = 0.06 rad/s (3.5 deg/s), and an ISAR image integration time t = 1s, the number of cross-range bins migrated is less than 1. In comparison, the distortion in the measured ISAR image for scatterer S_B as shown in Figure 7a is smeared over about 15 cross-range bins. The estimate on the quadratic distortion is, in fact, already a worse case scenario. A conservative value $|\omega_c|_{max}$ is used, even though a target with a fluctuating motion does not sustain this maximum value for the duration of time t. Moreover, the quadratic distortion is proportional to t^2. That is to say, the distortion increases with the image integration time. Even when t is increased to 3 seconds, the number of cross-range bins migrated is 6 according to Equation (20). This is still considerably less than the measured distortion of more than 40 cross-range bins as shown in Figure 8a. The increase in the number of bins in the measured ISAR images between Figures 7a and 8a is due to an increase in the cross-range resolution by integrating over a larger number of HRR profiles, which is proportional to the increase in the integration time t.

5. Restoration of Distorted ISAR Images

For target recognition applications, ISAR images of targets must have adequate spatial resolution. According to the principles of ISAR imaging, large radar bandwidth and long image integration time are required to produce fine image resolution. However, a long image integration time does not always guarantee good cross-range resolution. This is illustrated in the discussion above where it is found that the amount of blurring caused by non-uniform target motion over the image integration period can be quite severe.

Time-frequency techniques have been used to "refocus" blurred ISAR images [5]. As seen from the discussion above, the blurring of ISAR images is a consequence of a time-varying Doppler frequency resulting from non-uniform motion of the target. By extracting an ISAR image of the target at a particular instance of time, a better focused image can be obtained because the target's motion can be considered as relatively uniform over a short duration. However, there will be a large number of time instances to deal with in most time-frequency processing. Thus, a large number of refocused ISAR images will emerge, corresponding to the number of time instances. For fast, efficient target recognition, it is desirable to make use of only the best refocused image. It is impractical to examine all available refocused ISAR images. Visual inspection manually over a large number of images, or even using an automated image search algorithm only adds complexity to the target recognition process.

A more objective and more efficient way to determine the optimum refocused ISAR image is possible, based on the insights obtained from the image distortion analysis conducted in this paper. That is to say, it is found from the experimental and numerical studies that the blurring is directly related to the instantaneous Doppler frequency of the target, and the amount of blurring is dependent on the amount of Doppler variation within the image integration duration. The temporal Doppler behaviour of the target can be characterized using time-frequency analysis. The time-frequency spectrogram in Figure 4a traces out the Doppler frequency as a function of time at the down-range bin where the scatterer S_B is located. There are 75 time instances in the spectrogram, covering 3 seconds of image integration time. It corresponds to the distorted ISAR image illustrated in Figure 8a. The spectrogram is computed using Short Time Fourier Transform (STFT) with a 0.4 s image integration time window (i.e., 800 HRR profiles). In other words, each time instance represents a 0.4s time segment. Thus it is more accurate to describe a time instance as a short duration of time rather than a precise point in time. For the purpose of illustrating the methodology on how an optimum refocused ISAR image can be found, this definition of a time instance is sufficient. The scaling of the frequency axis in the spectrogram in Figure 4a is arbitrary. The frequency value 1 in this case corresponds to the zero Doppler frequency line (see Figure 4b).

Before discussing how an optimum refocused ISAR image can be determined, it is useful to take a look at samples of the refocused images at various time instances. A

refocused ISAR image is reconstructed from the spectrograms of all the down-range bins at a chosen time instance. Figure 10 shows the refocused ISAR images of the target at 6 time instances as indicated in Figure 4a. The ISAR image at time t_a corresponds to the instance when the target has an uniform rotational motion. This image serves as a reference image for comparing with the refocused images at other time instances. Using a 0.4s STFT, the resolution is just barely adequate to resolve the scatterers on the target in the cross-range direction for the uniform rotation case at t_a. A quick inspection of Figure 10 reveals that the best refocused image is at the time instance t_e and the worst images are at t_c and t_d.

By understanding why the images are the worst at t_c and t_d and why the image is the best at t_e, we can develop an objective methodology on how to reconstruct the optimum refocused ISAR image. The ISAR image at t_c appears compressed. This is due to the small Doppler frequency (i.e., small angular rotational rate) of the target at this time instance. It is even smaller than the uniform rotation case at t_a; this is illustrated in Figure 4b. The Doppler motion is too small to separate the scatterers adequately in the cross-range direction. The ISAR image at time t_d still appears blurry, with some of the scatterers still not properly focused. This is attributed to the fact that the Doppler motion of the target is going through a large temporal rate of change within this time instance, i.e., $\Delta f/\Delta t$ is large. The STFT window for the time instance t_d is indicated by the window slot as shown in Figure 4b. It can be seen that there is a large variation in the value of the Doppler frequency within the time instance t_d. We have seen from Sections 3 and 4 above that this large variation in the Doppler motion gives rise to a blurred image.

The ISAR image at t_e has all six scatterers on the target clearly resolved and provides the best refocused image. There are two reasons why the best image quality is found at time instance t_e. Firstly, the Doppler motion is large, significantly larger than the uniform rotational rate case at the time instance t_a (see Figure 4b). Hence the scatterers are much better separated by the large angular rotational rate in the cross-range. Secondly, the temporal rate of change of the Doppler motion in the time interval at t_e is small; i.e., $\Delta f/\Delta t$ is small. Therefore, the blurring to the image of the scatterer is kept to a minimum. The STFT window for time instance t_e is indicated in Figure 4b. It can be seen that the Doppler motion varies very little within time instance t_e.

Based on the analysis of the refocused images shown in Figure 10, we have deduced a few simple physical rules that will enable us to extract a relatively well focused image from a blurred ISAR image:

1. From the blurred image, locate a down-range bin where it contains the most severe blurring in the cross-range.
2. Produce a time-frequency spectrogram at the chosen down-range bin, using Short-Time Fourier transform or time-frequency distribution functions [6].
3. From the spectrogram, select a time instance when the variation of the Doppler motion is small (i.e., small $\Delta f/\Delta t$) and the the value of the

Doppler motion is large (i.e., as far away from the zero Doppler frequency as possible).

4. Construct spectrograms at all down-range bins from the blurred ISAR image that contain the target. Recombine the same time instance from all spectrograms to reconstruct a focused ISAR image.

This procedure provides a much faster means of constructing an optimum refocused image. This is because once the appropriate time instance is determined, only one ISAR image needs to be reconstructed. This is obviously much more efficient than extracting ISAR images at all time instances from all spectrograms because the number of time instances is usually very large. Another interesting note is that having a large amount of blurring in the ISAR image may actually be better than having just a small amount of blurring for restoring a focused image. A more severe blurring means that at some time instance, there is a large Doppler motion that can be exploited to get a better resolved image.

6. Conclusions

We have demonstrated experimentally that the ISAR images of a target can suffer large distortion when the target possesses a time-varying perturbed motion during the image integration period. The large distortion is attributed to the modulation effect in the phase of the return signal of a target with fluctuating motion. This results in blurring in the cross-range direction of the ISAR image due to a time-varying Doppler velocity from the fluctuating motion. The size of the distortion is determined by the amount of variation in the Doppler motion occurred during the imaging duration and is independent of the length of the image integration time.

A numerical model of the distortion process has been developed and has shown to be capable of predicting accurately the amount and the characteristics of the distortion in the ISAR images. The numerical predictions are validated by experimental data. The model results indicate that the phase modulation effect is the dominant mechanism for introducing the large distortion in the ISAR image of a moving target. This phase modulation effect can be modelled properly by including the temporal variation of the target's motion in its angular rotational rate. That is to say, the angular rotational velocity must be described as a function of time; i.e., $\omega(t)$ so that an instantaneous Doppler velocity can be ascribed at any given time. This permits the model to compute the amount of change in the Doppler motion over the duration of the image integration period, thus determining the amount of distortion in the ISAR image.

For target recognition applications, the blurred ISAR images of a moving target must be refocused in order to provide an usable image for identification. The numerical and experimental studies conducted in this report offer some useful insights and a better understanding of the distortion phenomenon in ISAR imaging. These findings allow us to develop an efficient procedure using time –frequency analysis to refocus the blurred ISAR images of moving targets.

Short-time Fourier transform is used in this report to demonstrate the refocusing capability of the time-frequency techniques for blurred ISAR images. Other time-frequency methods such as the Wigner-Ville distribution function and Choi-William distribution function are also widely used for image refocusing of moving targets. In brief, the work described here offers a means to improve on the target recognition process of moving targets such as in-flight aircraft and maneuvering ground vehicles and naval vessels. This work is especially relevant and pertinent to the ISAR imaging capability of the surveillance radar systems on-board of the CF C-140 Aurora patrol aircraft and the US Navy's P3 Orion surveillance aircraft. It should also be noted that target recognition based on radar imagery will play an important role in future CF initiatives on ISR (Intelligence, Surveillance and Reconnaissance) for land, air and maritime applications.

7. Figures

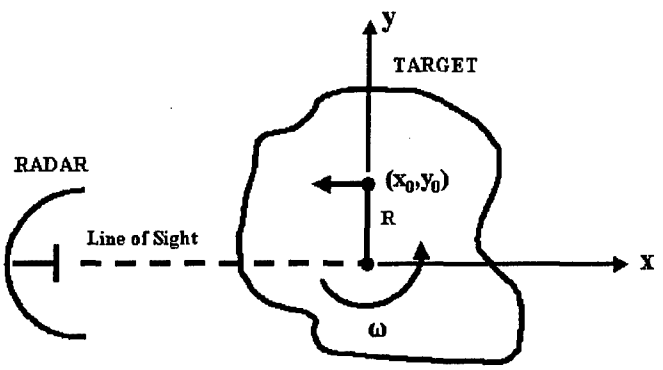

Figure 1 Schematic of a scatterer on a 2-dimensional target

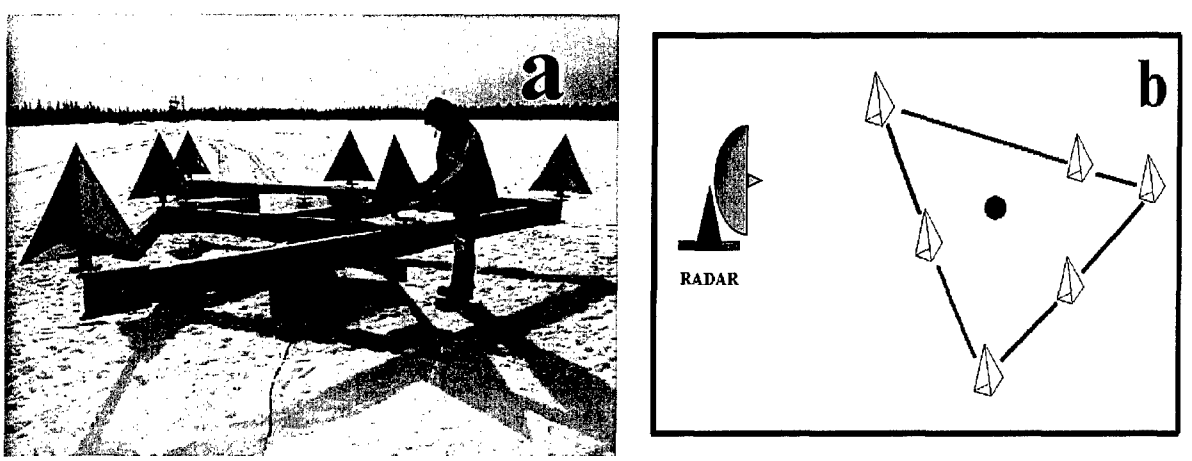

Figure 2 a) a picture of the target motion simulator; b) a schematic of the experimental set-up.

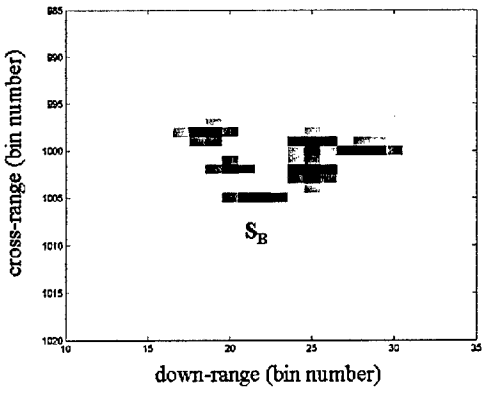

Figure 3 An undistorted ISAR image of the target recorded experimentally. Image integration time = 1 second.

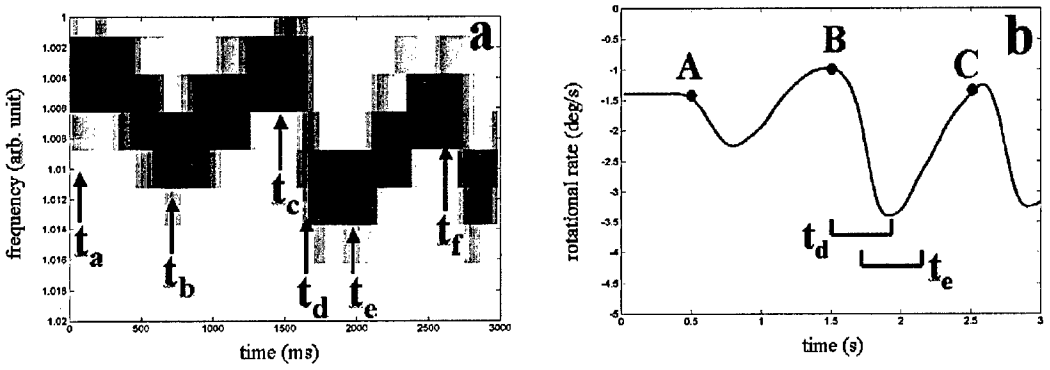

Figure 4 Temporal history of the relative movement of the scatterer S_B under an oscillating motion. a) time-frequency spectrogram, b) digitized trace.

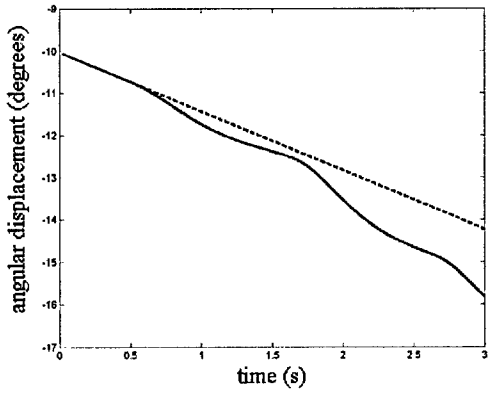

Figure 5 Angular displacement of the target as a function of time. Solid line = target with an oscillating motion superimposed on a constant rotation as illustrated in Figure 4; dashed line = target with a constant rotation at 1.4 degrees/s.

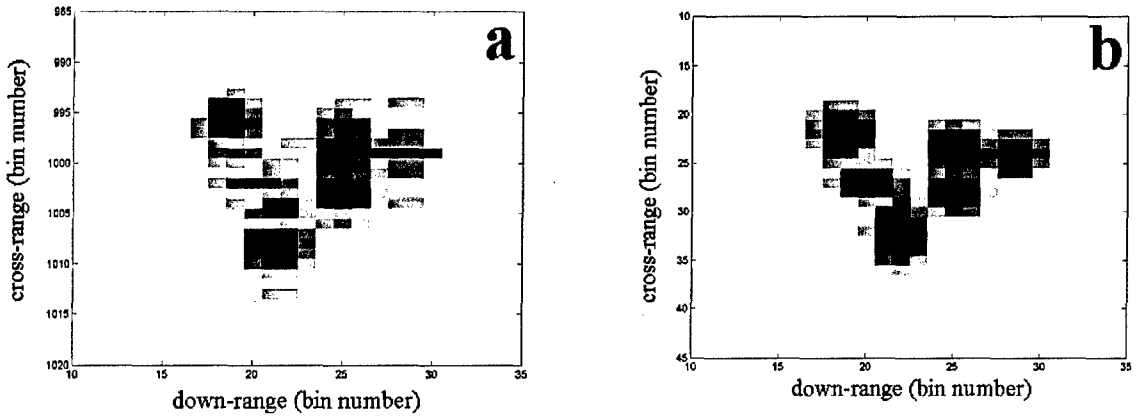

Figure 6 Distorted ISAR images. a) measured, b)simulated. Image integration time = 1 second, corresponding to the interval A to B in Figure 4b.

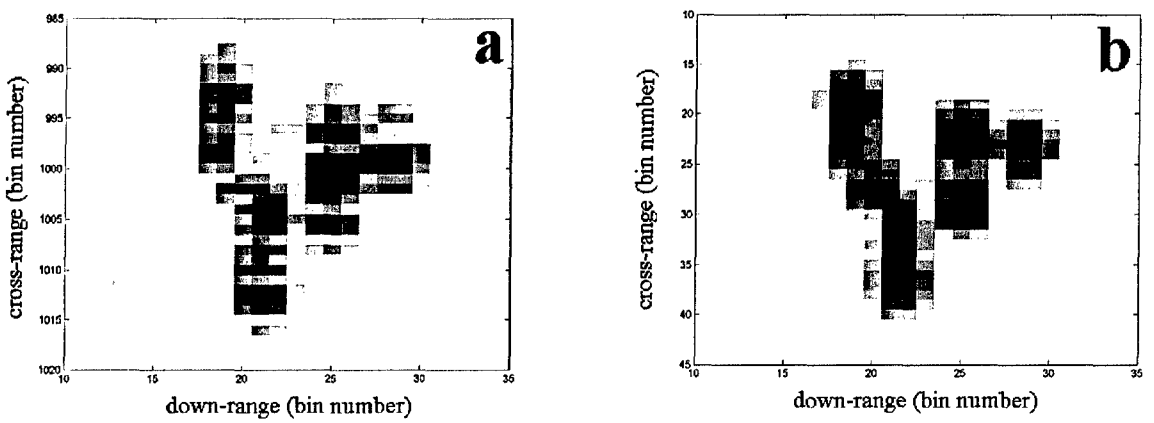

Figure 7 Distorted ISAR images. a) measured, b) simulated. Image integration time = 1second, corresponding to the interval B to C in Figure 4b.

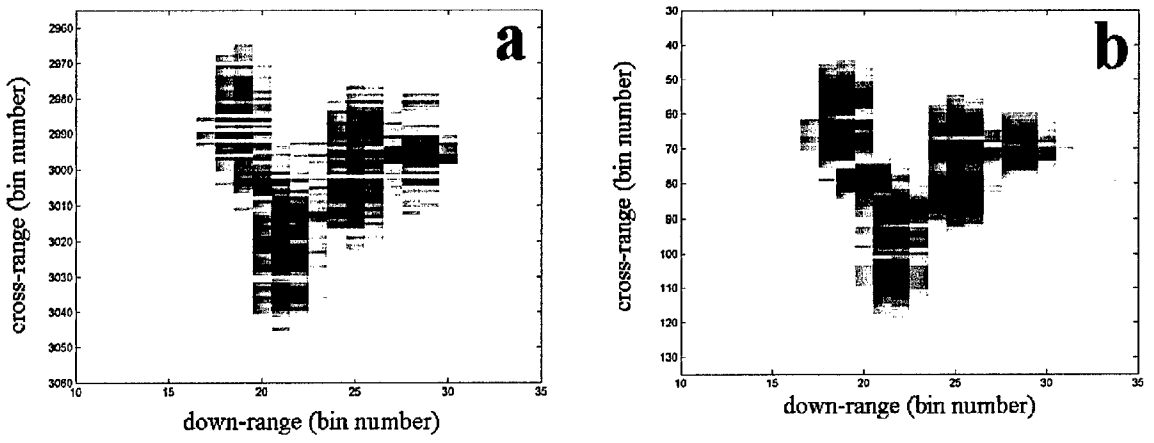

Figure 8 Distorted ISAR images. a) measured, b) simulated. Image integration time = 3 seconds as illustrated in Figure 4b.

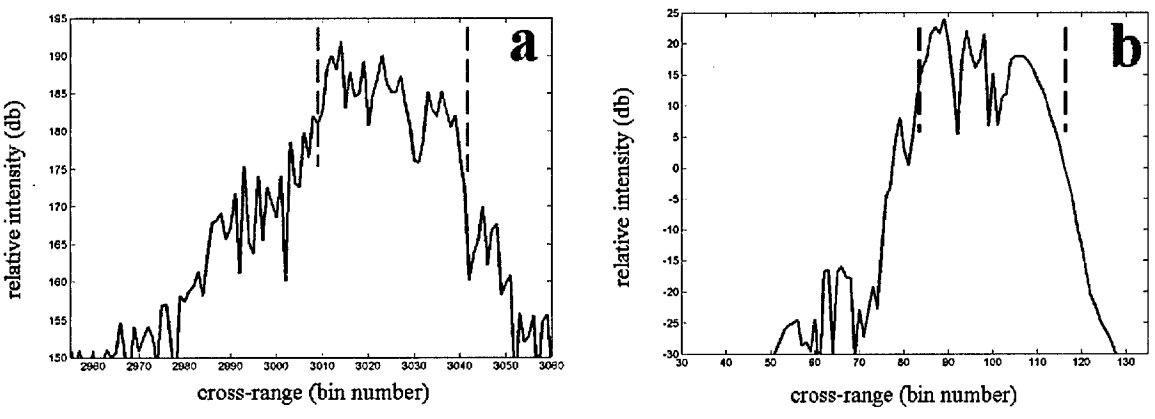

Figure 9 Intensity profile from a slice of the ISAR image (from Figure 8) in the cross-range direction at the location corresponding to scatterer S_B. a) measured, b) simulated. The width between the dashed lines denotes the blurring of the ISAR image of the scatterer S_B.

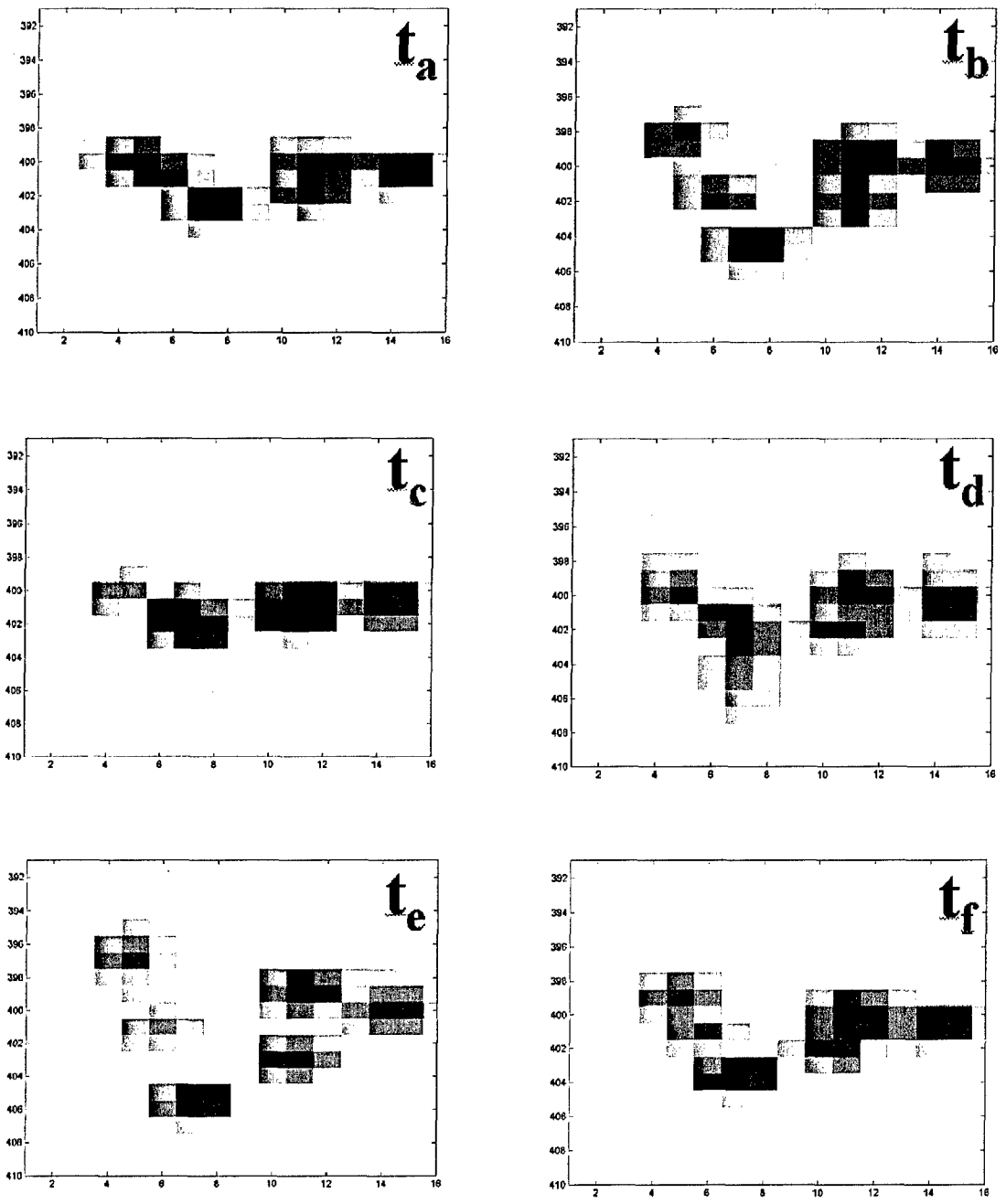

Figure 10 Reconstructed ISAR images from the blurred image (measured) as shown in Figure 8a, at various time instances as indicated in Figure 4a.

References

1. T. Sparr, S-E. Hamran and E. Korsbakken, "Estimation and Correction of Complex Target Motion Effects in Inverse Synthetic Aperture Imaging of Aircraft", IEEE Radar 2000 Conference, pp.457-462, USA, May 2000.

2. V. C. Chen and W. J. Miceli, "Simulation of ISAR imaging of moving Target", IEE Proc. - Radar, Sonar and Navigation, Vol. 148, No.3, pp.160-166, June 2001.

3. S. K. Wong, G. Duff and E. Riseborough, "Analysis of Distortion in the High Range Resolution Profile from a Perturbed Target", IEE Proc. - Radar, Sonar and Navigation, Vol.148, No.6, pp.353-362, December 2001.

4. D. Wehner, "High Resolution Radar", Artech House, Boston, 1987.

5. V. C. Chen and H. Ling, "Time-Frequency Transform for Radar Imagery and Signal Analysis", Artech House, Boston, 2002.

6. L. Cohen, "Time-Frequency Distributions - A Review", Proceedings of the IEEE, Vol.77, No.7, pp.941-980, July 1989.

DOCUMENT CONTROL DATA

(Security classification of title, body of abstract and indexing annotation must be entered when the overall document is classified)

1. ORIGINATOR (the name and address of the organization preparing the document. Organizations for whom the document was prepared, e.g. Establishment sponsoring a contractor's report, or tasking agency, are entered in section 8.)

Defence R&D Canada - Ottawa
Otawa, ON Canada K1A 0Z4

2. SECURITY CLASSIFICATION (overall security classification of the document, including special warning terms if applicable)

UNCLASSIFIED

3. TITLE (the complete document title as indicated on the title page. Its classification should be indicated by the appropriate abbreviation (S,C or U) in parentheses after the title.)

Distorttion in ISAR Imaging and Restoration of Distorted ISAR Images (U)

4. AUTHORS (Last name, first name, middle initial)

Wong, S., Duff, G., Riseborough, E.

5. DATE OF PUBLICATION (month and year of publication of document)	6a. NO. OF PAGES (total containing information. Include Annexes, Appendices, etc.)	6b. NO. OF REFS (total cited in document)
September 2003	29	6

7. DESCRIPTIVE NOTES (the category of the document, e.g. technical report, technical note or memorandum. If appropriate, enter the type of report, e.g. interim, progress, summary, annual or final. Give the inclusive dates when a specific reporting period is covered.)

Technical Memorandum

8. SPONSORING ACTIVITY (the name of the department project office or laboratory sponsoring the research and development. Include the address.)

Defence R&D Canada - Ottawa
3701 Carling Ave. Ottawa ON Canada K1A 0Z4

9a. PROJECT OR GRANT NO. (if appropriate, the applicable research and development project or grant number under which the document was written. Please specify whether project or grant)	9b. CONTRACT NO. (if appropriate, the applicable number under which the document was written)
11ar20	

10a. ORIGINATOR'S DOCUMENT NUMBER (the official document number by which the document is identified by the originating activity. This number must be unique to this document.)	10b. OTHER DOCUMENT NOS. (Any other numbers which may be assigned this document either by the originator or by the sponsor)
DRDC Ottawa TM 2003-143	

11. DOCUMENT AVAILABILITY (any limitations on further dissemination of the document, other than those imposed by security classification)

(X) Unlimited distribution
( ) Distribution limited to defence departments and defence contractors; further distribution only as approved
( ) Distribution limited to defence departments and Canadian defence contractors; further distribution only as approved
( ) Distribution limited to government departments and agencies; further distribution only as approved
( ) Distribution limited to defence departments; further distribution only as approved
( ) Other (please specify):

12. DOCUMENT ANNOUNCEMENT (any limitation to the bibliographic announcement of this document. This will normally correspond to the Document Availability (11). However, where further distribution (beyond the audience specified in 11) is possible, a wider announcement audience may be selected.)

13. ABSTRACT (a brief and factual summary of the document. It may also appear elsewhere in the body of the document itself. It is highly desirable that the abstract of classified documents be unclassified. Each paragraph of the abstract shall begin with an indication of the security classification of the information in the paragraph (unless the document itself is unclassified) represented as (S), (C), or (U). It is not necessary to include here abstracts in both official languages unless the text is bilingual).

Gross distortion on ISAR images due to small perturbed target motion is experimentally verified. Quantitative results obtained under controlled experimental conditions on the target's motion have confirmed that large distortion in the ISAR image of the target can occur. The distortion is a consequence of the phase modulation effect in the radar return signal, as a result of small fluctuating perturbed motion of the target. This gives rise to distortion of the image in the cross-range direction. The distortion can be refocused by applying time-frequency analysis. The Short-Time Fourier transform is used in this paper to examine some of the issues in refocusing distorted ISAR images.

14. KEYWORDS, DESCRIPTORS or IDENTIFIERS (technically meaningful terms or short phrases that characterize a document and could be helpful in cataloguing the document. They should be selected so that no security classification is required. Identifiers such as equipment model designation, trade name, military project code name, geographic location may also be included. If possible keywords should be selected from a published thesaurus. e.g. Thesaurus of Engineering and Scientific Terms (TEST) and that thesaurus-identified. If it is not possible to select indexing terms which are Unclassified, the classification of each should be indicated as with the title.)

ISAR Imaging, image distortion, Doppler motion, time-frequency analysis, short-time Fourier transform.

Defence R&D Canada

Canada's leader in defence
and national security R&D

R & D pour la défense Canada

Chef de file au Canada en R & D
pour la défense et la sécurité nationale

DEFENCE R&D DÉFENSE

www.drdc-rddc.gc.ca